cmgh
CELLULAR AND MOLECULAR GASTROENTEROLOGY AND HEPATOLOGY

ORIGINAL RESEARCH

Hypoxia via ERK Signaling Inhibits Hepatic PPARα to Promote Fatty Liver

Raja Gopal Reddy Mooli,[1] Jessica Rodriguez,[2] Shogo Takahashi,[3,4] Sumeet Solanki,[2] Frank J. Gonzalez,[4] Sadeesh K. Ramakrishnan,[1,2] and Yatrik M. Shah[2]

[1]Division of Endocrinology and Metabolism, Department of Medicine, University of Pittsburgh, Pittsburgh, Pennsylvania; [2]Department of Molecular and Integrative Physiology, Internal Medicine, University of Michigan, Ann Arbor, Michigan; [3]Departments of Biochemistry and Molecular and Cellular Biology, Georgetown University, Washington, District of Columbia; and [4]National Cancer Institute, National Institutes of Health, Bethesda, Maryland

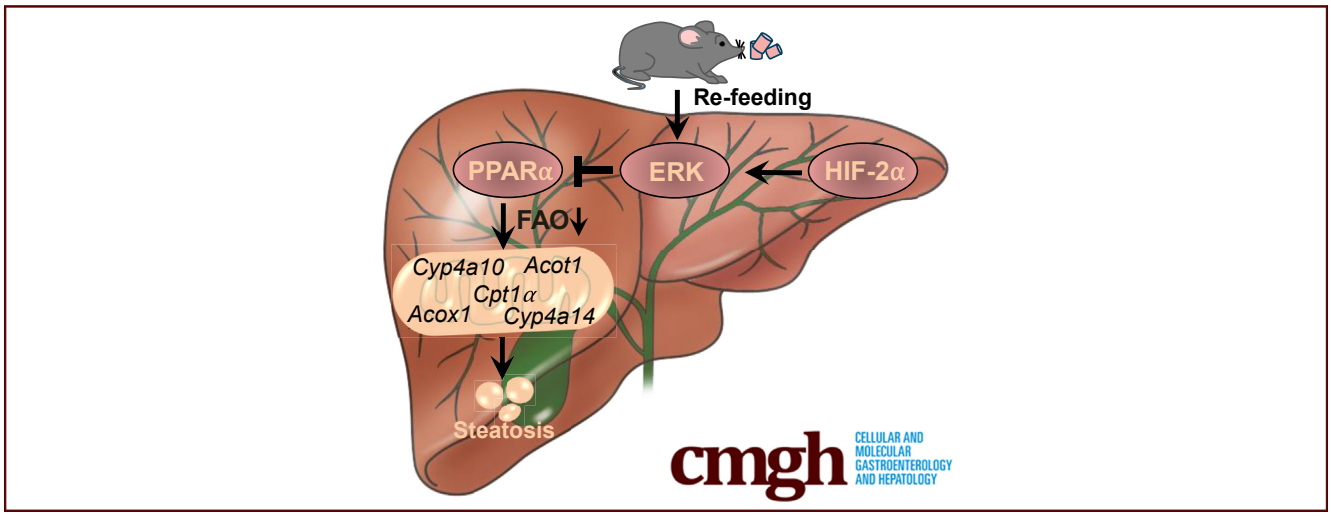

SUMMARY

Hypoxia-inducible factor (HIF)2α promotes NAFLD progression by repressing genes involved in fatty acid β-oxidation through unclear mechanisms. Here we demonstrate that HIF2α promotes hepatic steatosis via ERK-mediated repression of PPARα activity. Furthermore, ERK regulation of PPARα is an essential mechanism involved in diet-induced hepatic steatosis and postprandial repression of fatty acid β-oxidation genes.

BACKGROUND & AIMS: Fatty liver or nonalcoholic fatty liver disease (NAFLD) is the most common liver disease associated with comorbidities such as insulin resistance and cardiovascular and metabolic diseases. Chronic activation of hypoxic signaling, in particular, hypoxia-inducible factor (HIF)2α, promotes NAFLD progression by repressing genes involved in fatty acid β-oxidation through unclear mechanisms. Therefore, we assessed the precise mechanism by which HIF2α promotes fatty liver and its physiological relevance in metabolic homeostasis.

METHODS: Primary hepatocytes from VHL ($Vhl^{\Delta Hep}$) and PPARα (*Ppara*-null) knockout mice that were loaded with fatty acids, murine dietary protocols to induce hepatic steatosis, and fasting-refeeding dietary regimen approaches were used to test our hypothesis.

RESULTS: Inhibiting autophagy using chloroquine did not decrease lipid contents in $Vhl^{\Delta Hep}$ primary hepatocytes. Inhibition of ERK using MEK inhibitor decreased lipid contents in primary hepatocytes from a genetic model of constitutive HIF activation and primary hepatocytes loaded with free fatty acids. Moreover, MEK-ERK inhibition potentiated ligand-dependent activation of PPARα. We also show that MEK-ERK inhibition improved diet-induced hepatic steatosis, which is associated with the induction of PPARα target genes. During fasting, fatty acid β-oxidation is induced by PPARα, and refeeding inhibits β-oxidation. Our data show that ERK is involved in the postprandial repression of hepatic PPARα signaling.

CONCLUSIONS: Overall, our results demonstrate that ERK activated by hypoxia signaling plays a crucial role in fatty acid β-oxidation genes by repressing hepatocyte PPARα signaling. *(Cell Mol Gastroenterol Hepatol 2021;12:585–597; https://doi.org/10.1016/j.jcmgh.2021.03.011)*

Keywords: ERK; MEK; PPARα; Hypoxia; HIF; Fatty Liver; β-Oxidation.

Fatty acid oxidation plays a pivotal role in energy homeostasis.[1] During fasting, fatty acids are transported to the liver, and metabolites derived from fatty acid catabolism serve as substrates for gluconeogenesis.[2] Mitochondria and peroxisomes play an essential role in

fatty acid β-oxidation,[3] and a defect in mitochondrial or peroxisomal metabolism results in dyslipidemia, leading to metabolic disorders.[4] During fasting, hepatic fatty acid β-oxidation is induced by the ligand-activated transcription factor peroxisome proliferator-activated receptor α (PPARα).[5] On refeeding, a rapid switch in metabolic flux from β-oxidation to carbohydrate metabolism is associated with attenuation of PPARα signaling through unclear mechanisms. In the refed state, hypoxia signaling is robustly induced in the liver.[6–9] Previously we demonstrated that hypoxia signaling inhibits PPARα activity; however, the precise link between hepatic hypoxia and PPARα in metabolic homeostasis remains unclear.

Hypoxia signaling is mediated by the transcription factors hypoxia-inducible factor (HIF) 1α and HIF2α.[10–13] In the liver, HIF2α but not HIF1α plays a crucial role in fatty liver disease.[8,9,14,15] Activation of HIF2α alters expression of genes involved in lipid metabolism, resulting in hypercholesterolemia and fatty liver.[8,15–17] HIF2α does not affect mitochondrial oxidative phosphorylation but instead suppresses the expression of numerous PPARα target genes involved in fatty acid β-oxidation.[7] In particular, studies have shown that activation of HIF2α signaling dramatically alters PPARα activity and decreases peroxisome numbers by inducing pexophagy.[7,18,19]

Here we sought to precisely define the mechanism by which HIF2α promotes fatty liver. We demonstrate that HIF2α-mediated activation of extracellular signal-regulated kinase (ERK) decreases PPARα activity. Inhibition of ERK decreases lipid content in primary hepatocytes via potentiation of PPARα activation and attenuates diet-induced hepatic steatosis. We further show that ERK regulation of PPARα is an essential mechanism involved in postprandial repression of genes involved in fatty acid β-oxidation.

Results

Inhibition of Autophagy Does not Ameliorate HIF-Mediated Lipid Accumulation

HIF2α was shown to induce hepatic steatosis by selective autophagic degradation of peroxisomes (pexophagy),[19] an organelle involved in fatty acid β-oxidation. To explore the role of autophagy in HIF-mediated hepatic steatosis, mice that express a Cre^{ERT2} under the control of the albumin promoter were used to spatially and temporally disrupt Von Hippel-Lindau (VHL) in hepatocytes ($Vhl^{\Delta Hep}$).[9,17] VHL is an E3 ubiquitin ligase that ubiquitinates and targets the α-subunit of HIF to proteolytic degradation under normoxic conditions.[20] Thus, disruption of VHL results in the stabilization of HIFs in the liver.[9] These mice exhibit robust liver steatosis in a HIF2α-dependent manner.[8,9] One week after tamoxifen treatment, primary hepatocytes were isolated from $Vhl^{\Delta Hep}$ and $Vhl^{fl/fl}$ mice. Consistent with the previous reports,[9,19] lipid accumulation was observed in $Vhl^{\Delta Hep}$ primary hepatocytes compared with $Vhl^{fl/fl}$ mice (Figure 1*A*). However, inhibiting autophagy using chloroquine did not decrease lipid contents in $Vhl^{\Delta Hep}$ primary hepatocytes (Figure 1*A*). Western blot analysis shows an increase in LC3-II levels upon chloroquine treatment, confirming efficient inhibition of autophagy in $Vhl^{\Delta Hep}$ and $Vhl^{fl/fl}$ primary hepatocytes (Figure 1*B*). However, inhibition of autophagy did not restore catalase expression, suggesting that autophagy does not regulate peroxisome content in $Vhl^{\Delta Hep}$ mice (Figure 1*B*). We and others previously demonstrated that HIF activation decreases PPARα signaling in the liver.[8,9,18] Consistently, the expression of PPARα and its target genes involved in fatty acid β-oxidation was decreased in $Vhl^{\Delta Hep}$ primary hepatocytes (Figure 1*B* and *C*). Chloroquine treatment decreased WY-mediated induction of fatty acid β-oxidation genes (Figure 1*C*), in agreement with recent studies showing that autophagy is required to induce genes involved in fatty acid β-oxidation.[21,22] Moreover, inhibiting autophagy decrease did not restore the expression of genes involved in fatty acid β-oxidation (Figure 1*B* and *C*). This suggests that increased pexophagy is not solely responsible for HIF-mediated lipid accumulation, and inhibition of autophagy does not rescue PPARα signaling in $Vhl^{\Delta Hep}$ primary hepatocytes.

Inhibition of ERK1/2 Ameliorates HIF-Mediated Lipid Accumulation

Hepatic glucagon signaling plays an essential role in triglyceride metabolism.[23,24] More importantly, glucagon signaling synergistically potentiates fatty acid oxidation via PPARα, and glucagon receptor knockout mice ($Gcgr^{-/-}$) have elevated fasting triglycerides and free fatty acids.[25,26] We previously demonstrated that activation of HIF2α inhibits hepatic glucagon signaling via ERK-mediated repression of protein kinase A (PKA)-CREB signaling.[6] To determine whether the MEK-ERK pathway is involved in HIF-mediated decrease in fatty acid β-oxidation, primary hepatocytes from $Vhl^{fl/fl}$ and $Vhl^{\Delta Hep}$ mice were treated with the MEK inhibitor trametinib (GSK1120212; GSK). Intriguingly, inhibition of MEK-ERK signaling using GSK restored the expression of genes involved in fatty acid β-oxidation such as acyl-coenzyme A oxidase *(Acox1)*, acyl-CoA thioesterase 1 *(Acot1)*, carnitine palmitoyltransferase 1 (*Cpt1a*), cytochrome P450 family 4 subfamily a, polypeptide 10 and 14 (*Cyp4a10* and *Cyp4a14*), fibroblast growth factor 21 (*Fgf21*), and cluster of differentiation 36 (*CD36*) in primary hepatocytes from $Vhl^{\Delta Hep}$ mice (Figure 2*A*). Activation of HIF inhibits PKA signaling,[6] a key signaling mechanism through which glucagon induces fatty acid β-oxidation. Our data show that

Abbreviations used in this paper: **Acot1, acyl-CoA thioesterase 1; Acox1, acyl-coenzyme A oxidase; CD36, cluster of differenatiation 36; Cpt1a, carnitine palmitoyltransferase 1; Cyp4a10 and Cyp4a14, cytochrome P450, family 4, subfamily a, polypeptide 10 and 14; ERK, extracellular signal-regulated kinase; Fgf21, fibroblast growth factor 21; HFD, high-fat diet; HIF1α and HIF2α, hypoxia inducing factor 1 and 2 alpha; NAFLD, nonalcoholic fatty liver disease; PKA, protein kinase A; PPARα, peroxisome proliferator activated receptor alpha; qPCR, quantitative polymerase chain reaction; VHL, Von Hippel-Lindau; WT, wild-type.**

Most current article

2352-345X
https://doi.org/10.1016/j.jcmgh.2021.03.011

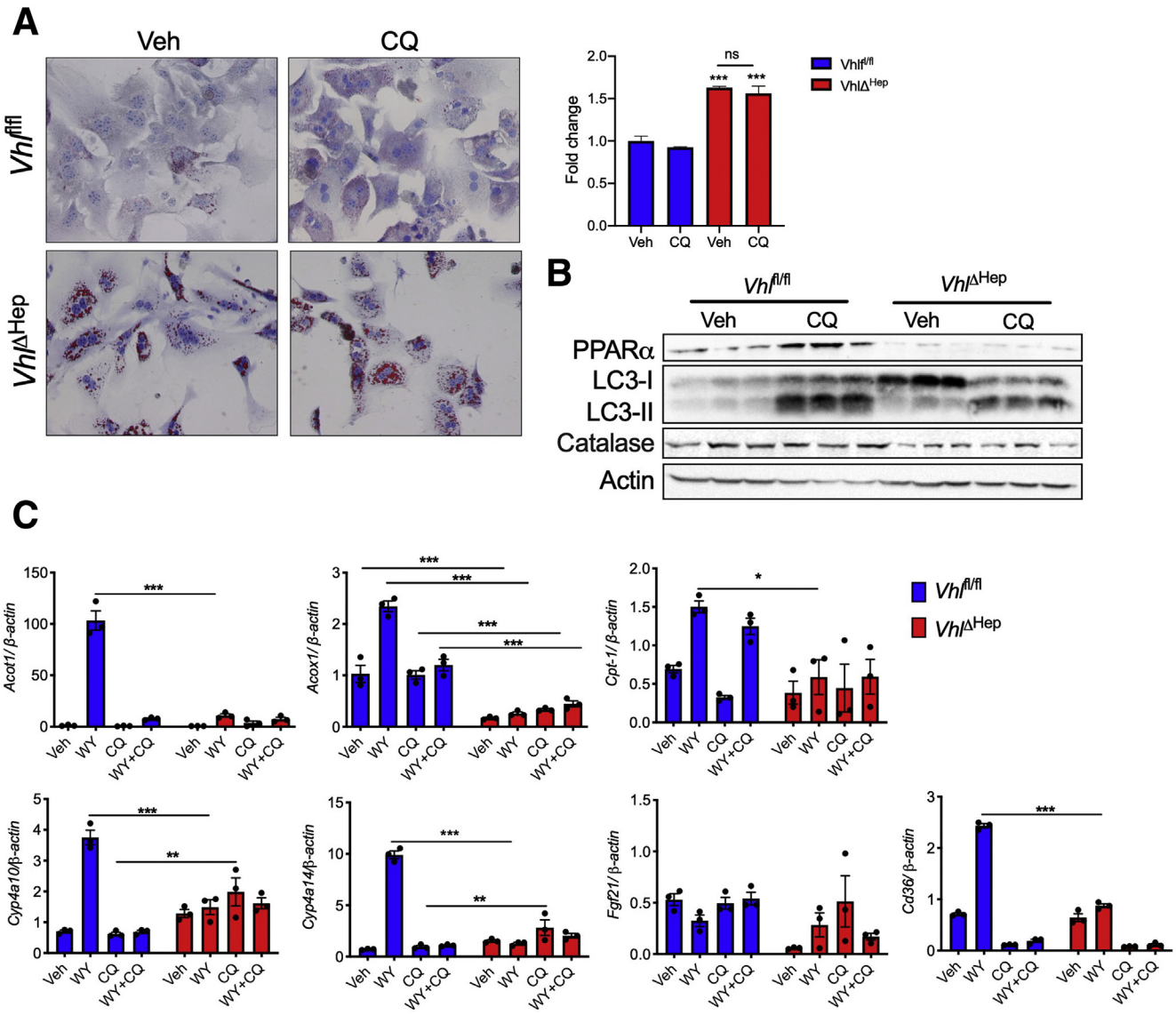

Figure 1. Inhibition of autophagy does not decrease lipid content in primary hepatocytes from *Vhl*$^{\Delta Hep}$ mice. (*A*) Oil-red-O staining and quantification (*right*) in primary hepatocytes from *Vhl*$^{fl/fl}$ and *Vhl*$^{\Delta Hep}$ mice treated with chloroquine (CQ; 10 μmol/L) for 16 hours. Original magnification, $\times$20. (*B*) Western blot analysis for PPARα, LC3B, and catalase in primary hepatocytes from *Vhl*$^{fl/fl}$ and *Vhl*$^{\Delta Hep}$ mice that were treated with 10 μmol/L CQ for 16 hours. (*C*) qPCR analysis for PPARα target genes in primary hepatocytes from *Vhl*$^{fl/fl}$ and *Vhl*$^{\Delta Hep}$ mice that were pretreated with or without 10 μmol/L CQ for 1 hour and then treated with the PPARα agonist 30 μmol/L WY14,643 (WY). Bar graphs presented as mean standard error $\pm$ standard error of the mean. $^{*}P < .05$, $^{**}P < .01$, $^{***}P < .001$ as analyzed by two-tailed *t* test. Veh, vehicle.

ERK inhibition increased expression of the genes involved in fatty acid β-oxidation in *Vhl*$^{\Delta Hep}$ primary hepatocytes, even in the presence of the PKA inhibitor (H89) (Figure 2*A*). Furthermore, inhibition of the MEK-ERK pathway ameliorated lipid accumulation in primary hepatocytes from *Vhl*$^{\Delta Hep}$ mice treated with the PKA inhibitor (Figure 2*B*). We then assessed whether GSK decreased hepatocyte lipid content by restoring PPARα expression. Our data show that the mRNA expression of fatty acid β-oxidation does not correspond with any significant increase in PPARα in *Vhl*$^{\Delta Hep}$ primary hepatocytes (Figure 2*C*). Together, these data suggest that ERK inhibition ameliorates HIF-mediated lipid accumulation by restoring fatty acid β-oxidation in a PKA-independent manner.

ERK Inhibition Decreases Fatty Acid-Induced Lipid Accumulation

We further tested whether inhibition of the MEK-ERK pathway could restore lipid accumulation in a model of fatty acid overload. Primary hepatocytes were serum-starved for 2 hours and then loaded with fatty acids for 16 hours. Fatty acid loading increased the levels of

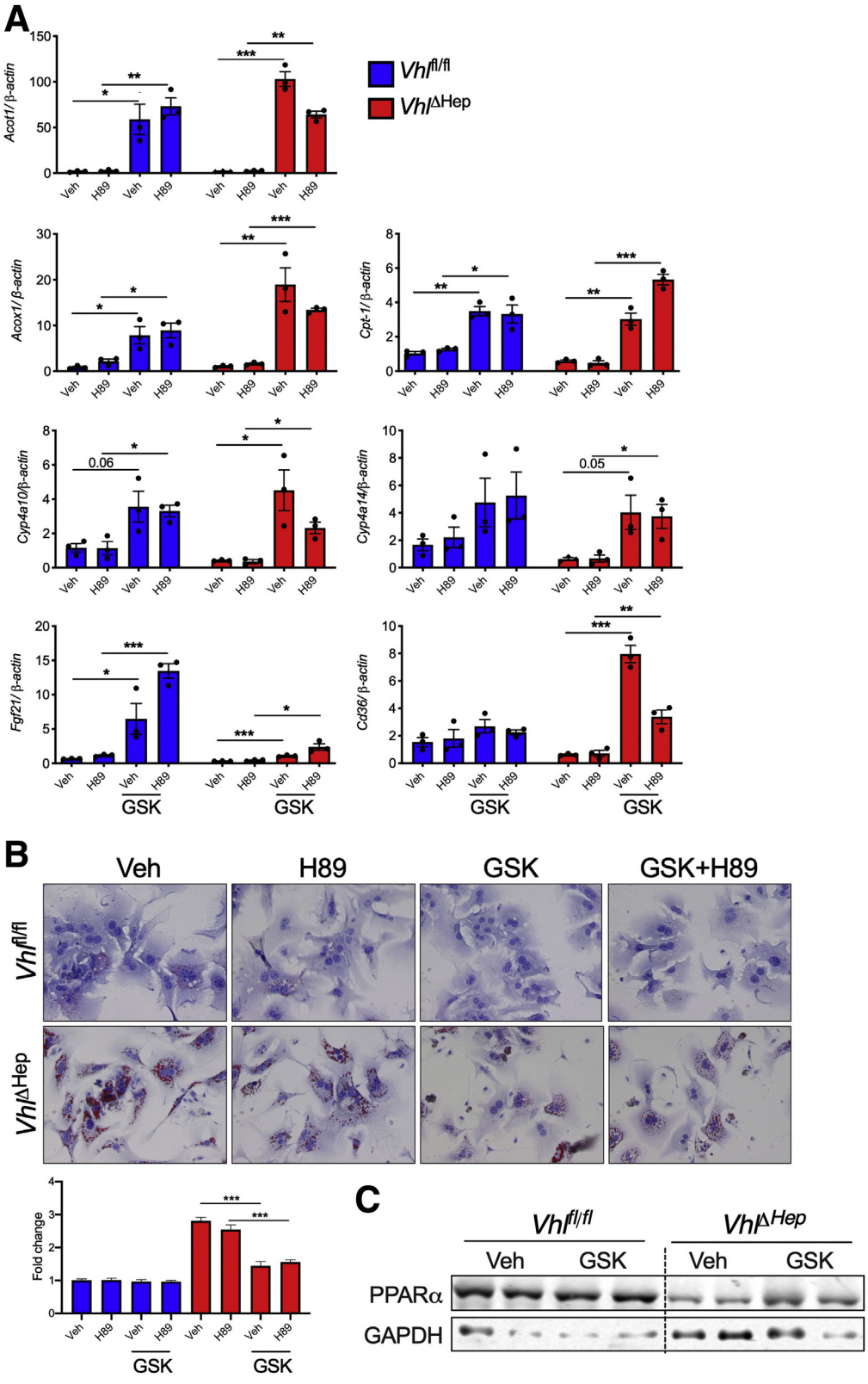

Figure 2. ERK inhibition induces PPARα target genes independent of PKA. (*A*) qPCR analysis for PPARα target genes and (*B*) oil-red-O staining for neutral lipids and quantification (*bottom*) in primary hepatocytes from $Vhl^{fl/fl}$ and $Vhl^{\Delta Hep}$ mice that were treated with Vehicle (Veh) or MEK inhibitor GSK1120212 (GSK; 0.5 μmol/L) for 16 hours in the presence or absence of PKA inhibitor H89 (0.5 μmol/L). (*C*) Western blot analysis for PPARα in $Vhl^{fl/fl}$ and $Vhl^{\Delta Hep}$ primary hepatocytes treated with 0.5 μmol/L GSK for 16 hours. Original magnification, ×20. Bar graphs are presented as mean standard error ± standard error of the mean. $^{*}P < .05$, $^{**}P < .01$, $^{***}P < .001$ as analyzed by two-tailed Student *t* test.

phosphorylated ERK in primary hepatocytes (Figure 3*A*), whereas MEK inhibitors (GSK and PD0325901) and ERK inhibitor (FR180204; FR) decreased expression and/or phosphorylation of ERK (Figure 3*A*). Notably, oil red-O staining revealed that inhibition of MEK-ERK signaling decreased lipid contents in fatty acid-loaded primary hepatocytes (Figure 3*B*). In addition, adenoviral-mediated knockdown of ERK1/2 in primary hepatocytes

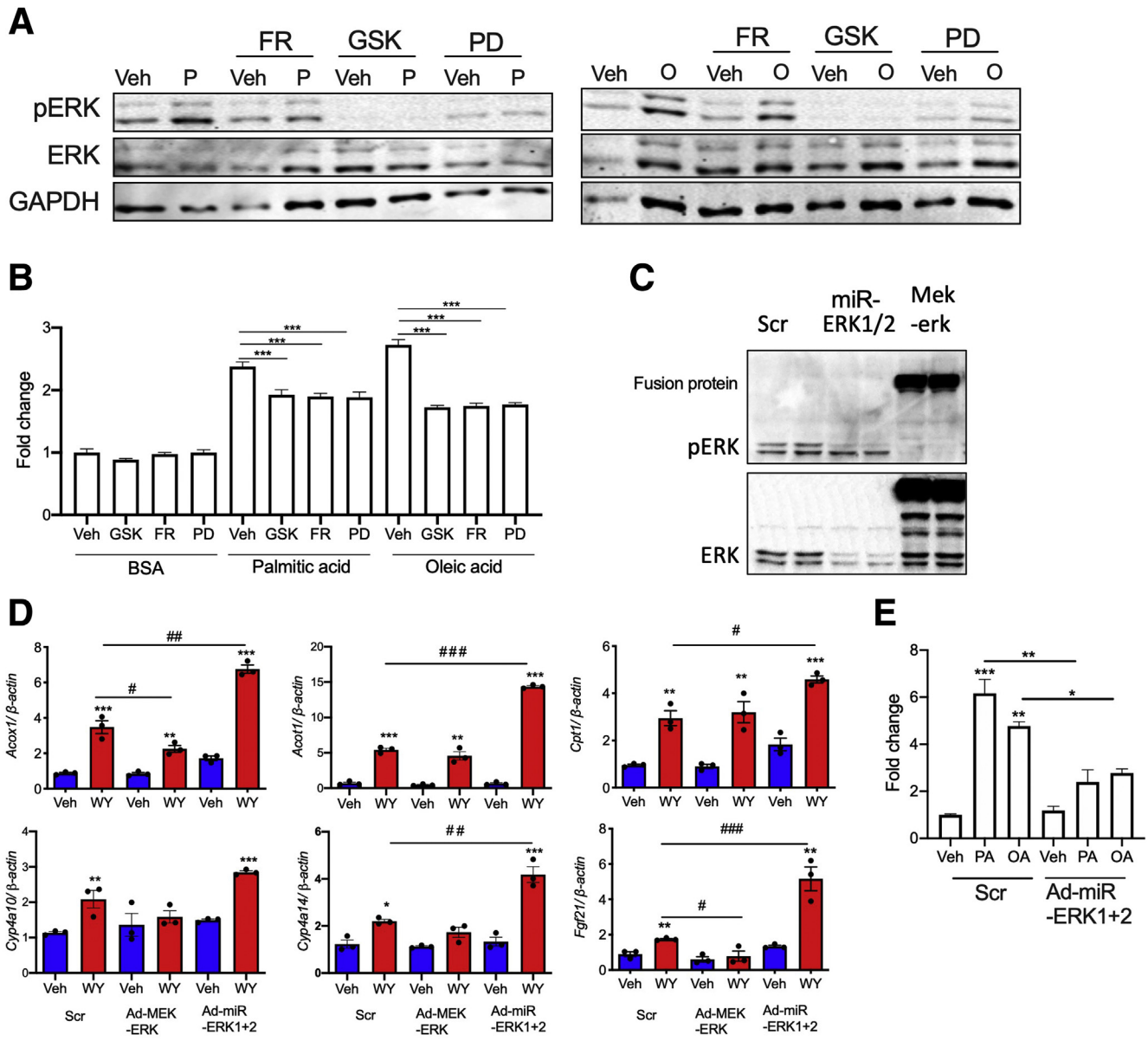

Figure 3. ERK inhibition attenuates fatty acid-induced lipid accumulation. (*A*) Western blot analysis for pERK in primary hepatocytes incubated with 100 μmol/L palmitic acid (P) or 200 μmol/L oleic acid in the presence of 0.5 μmol/L GSK or PD0325901 (PD) or ERK inhibitor (0.5 μmol/L FR180204; FR) for 16 hours. (*B*) Quantification of oil-red-O staining in primary hepatocytes treated with palmitic acid (100 μmol/L) or oleic acid (200 μmol/L) in the presence of MEK or ERK inhibitors. (*C*) Western blot analysis showing knockdown of ERK or overexpression of constitutively active MEK-ERK fusion protein in primary hepatocytes injected with adenovirus harboring LacZ (Scr), miR-ERK1/2, or fused MEK-ERK gene. (*D*) qPCR analysis for ligand-mediated induction of fatty acid oxidation-related genes in primary hepatocytes infected with Ad-MEK-ERK or Ad-miR-ERK1/2. (*E*) Quantification of oil-red-O staining in primary hepatocytes infected with Ad-MEK-ERK or Ad-miR-ERK1/2. Bar graphs are presented as mean standard error ± standard error of the mean. #$P < .05$, **$P < .01$, ##$P < .01$, ***$P < .001$, ###$P < .001$ as analyzed by one-way analysis of variance with Tukey multiple comparison. * represents the difference between Veh and other groups, and # represents the difference within the groups.

potentiated and overexpression of constitutively active ERK attenuated ligand-mediated induction of PPARα target gene mRNAs (Figure 3*C* and *D*). Moreover, knockdown of ERK1/2 decreased the lipid content in fatty acid-loaded primary hepatocytes (Figure 3*E*). Together, these data show that ERK inhibition attenuates lipid accumulation in a primary hepatocyte model of fatty acid overload.

MEK-ERK Inhibition Potentiates Ligand-Dependent PPARα Activity

MEK binding induces nuclear exclusion of PPARα and thereby inhibits PPARα signaling.[27] Other reports also suggest a direct role for ERK in regulating PPARα.[27,28] To determine whether MEK-ERK pathway regulates the basal or ligand-dependent PPARα activation, primary hepatocytes

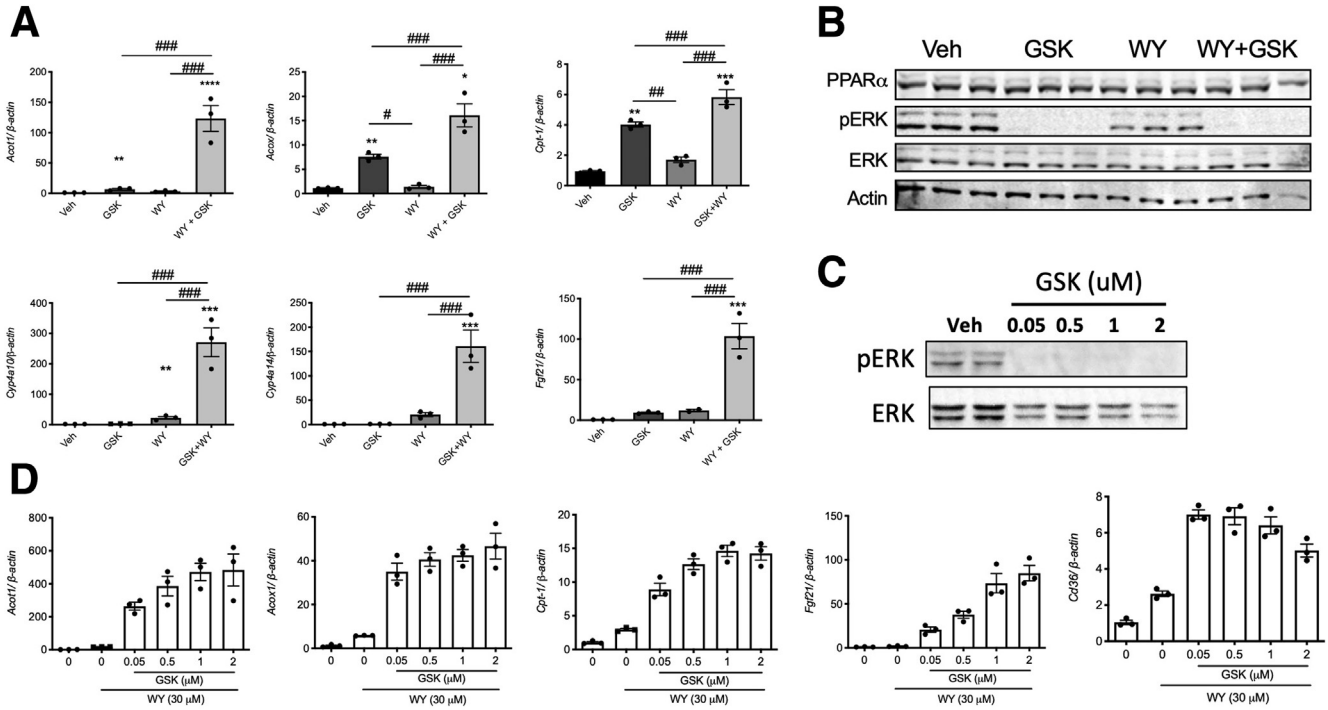

Figure 4. ERK inhibition augments ligand-mediated PPARα activation. (*A*) qPCR analysis assessing ligand-stimulated PPAR target genes in the presence or absence of 0.5 μmol/L GSK for 16 hours. (*B*) Western blot analysis for PPARα and pERK in primary hepatocytes from WT mice. (*C*) Western blot of pERK in primary hepatocytes treated with increasing dose of MEK inhibitor GSK. (*D*) qPCR analysis assessing dose-dependent effect of MEK inhibitor GSK on ligand-mediated induction of PPARα target genes. Bar graphs are presented as mean standard error ± standard error of the mean. *$P < .05$, #$P < .05$, **$P < .01$, ##$P < .01$, ***$P < .001$, ###$P < .001$ as analyzed by one-way analysis of variance with Tukey multiple comparisons. * represents the difference between Veh and other groups, and # represents the difference within the groups.

from wild-type (WT) mice were treated with the PPARα agonist WY14,643 (WY) in the presence or absence of GSK. ERK inhibition potentiated the WY-mediated increases in PPARα target gene mRNA expression in primary hepatocytes (Figure 4*A*). However, ERK inhibition did not affect PPARα protein levels, suggesting that ERK inhibits PPARα transactivation (Figure 4*B*). We also noticed a dose-dependent increase in ligand-mediated activation of PPARα upon ERK inhibition (Figure 4*C* and *D*). Together, these data suggest that MEK-ERK acts as a negative regulator of PPARα signaling.

PPARα Is Essential for ERK Regulation of Genes Involved in Fatty Acid β-Oxidation

To further determine whether ERK regulates fatty acid β-oxidation via PPARα, primary hepatocytes from *Ppara*-null mice were examined. Treatment with GSK significantly increased WY-mediated PPARα activation in primary hepatocytes from WT but not *Ppara*-null mice (Figure 5*A*). Moreover, overexpression of MEK-ERK fusion protein decreased and knockdown of ERK increased the expression of fatty acid β-oxidation genes in WT but not *Ppara*-null mice (Figure 5*B*). Furthermore, GSK treatment decreased lipid accumulation in primary hepatocytes from WT but not *Ppara-null* mice (Figure 5*C*). Together, these data show that ERK regulates hepatic fatty acid metabolism via a PPARα-dependent mechanism.

ERK Inhibition Attenuates Hepatic Steatosis

We then tested whether inhibition of the MEK-ERK pathway could ameliorate hepatic steatosis in a mouse model of diet-induced obesity. Mice fed a 60% high-fat diet (HFD) for 8 weeks were gavaged with GSK for 5 consecutive days. Inhibition of MEK-ERK signaling resulted in a significant reduction in body weight (Figure 6*A*). Also, a decrease in the liver weight (Figure 6*B*) but no difference in the visceral adiposity were noted (Figure 6*C*). GSK treatment resulted in a significant decrease in the serum and liver triglycerides (Figure 6*D* and *E*). Moreover, H&E analysis showed a significant reduction in microsteatosis and macrosteatosis in GSK-treated HFD-fed mice (Figure 6*F*). This suggests that inhibition of MEK-ERK attenuated hepatic steatosis. Further analysis by quantitative polymerase chain reaction (qPCR) showed a significant increase in the expression of PPARα target genes in the livers of GSK-treated HFD-fed mice (Figure 6*G*). However, no difference in *Cpt1*, *FGF21,* and *Cd36* was noted (Figure 6*G*). Thus, our data suggest that inhibition of the MEK-ERK pathway induces PPARα signaling and attenuates hepatic steatosis in a diet-induced obese model.

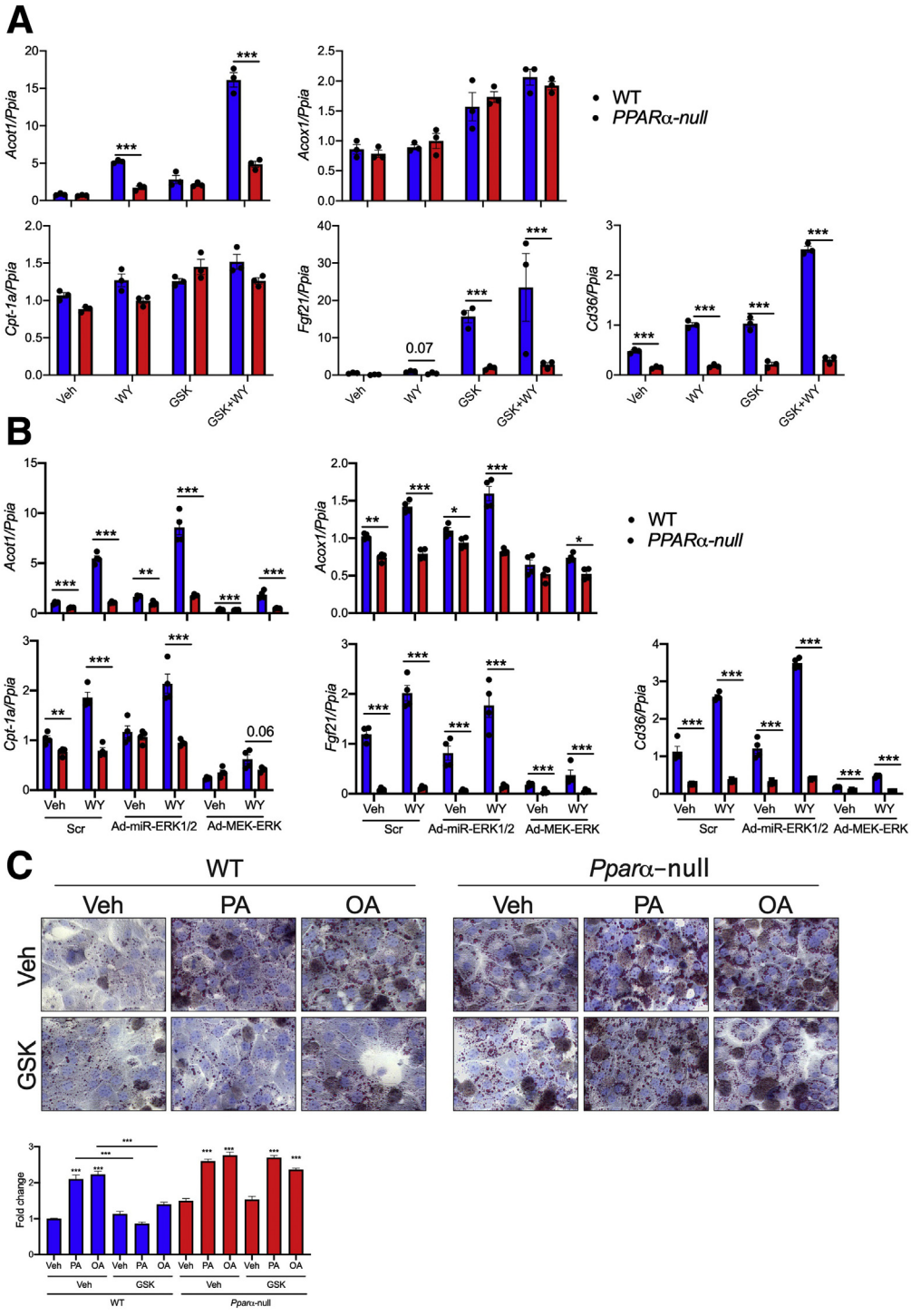

Figure 5. ERK regulates fatty oxidation gene mRNAs via PPARα. (*A*) qPCR analysis for ligand-mediated induction of PPARα target gene mRNAs in primary hepatocytes from WT or *Ppara-null* mice infected with Scr (Ad-LacZ) or Ad-miR-ERK1/2 or Ad-MEK-ERK. (*B*) qPCR analysis assessing effect of MEK inhibition on ligand-mediated induction of PPARα target genes in primary hepatocytes from WT or *Ppara*-null mice. (*C*) Oil-red-O staining and quantification (*below*) in primary hepatocytes loaded with 100 μmol/L palmitic (PA) and 100 μmol/L oleic acid (OA) for 24 hours, followed by treatment with 0.5 μmol/L GSK for 16 hours. Original magnification, ×20. Bar graphs are presented as mean standard error ± standard error of the mean. **P* < .05, ***P* < .01, ****P* < .001 as analyzed by two-tailed Student *t* test.

ERK Regulates Postprandial Repression of PPARα Activity

During fasting and refeeding, the liver plays a central role in energy homeostasis via PPARα-mediated fatty acid metabolism.[29] Refeeding is an energy rich state, with metabolic flux favoring glucose metabolism over fatty acid β-oxidation, enabling restoration of hepatic glycogen. Therefore, PPARα activity is rapidly repressed under the refed state through mechanisms that are not well-understood.[30] To investigate whether ERK is the postprandial regulator of PPARα, the expression of PPARα target genes was examined in livers of overnight fasted and refed mice treated with or without GSK (Figure 7*A*). Surprisingly, MEK-ERK inhibition under fasting conditions did not affect the expression of genes involved in hepatic fatty acid β-oxidation. However, MEK-ERK inhibition during the refed state abolished the postprandial decrease in expression of numerous PPARα target gene mRNAs related to fatty acid

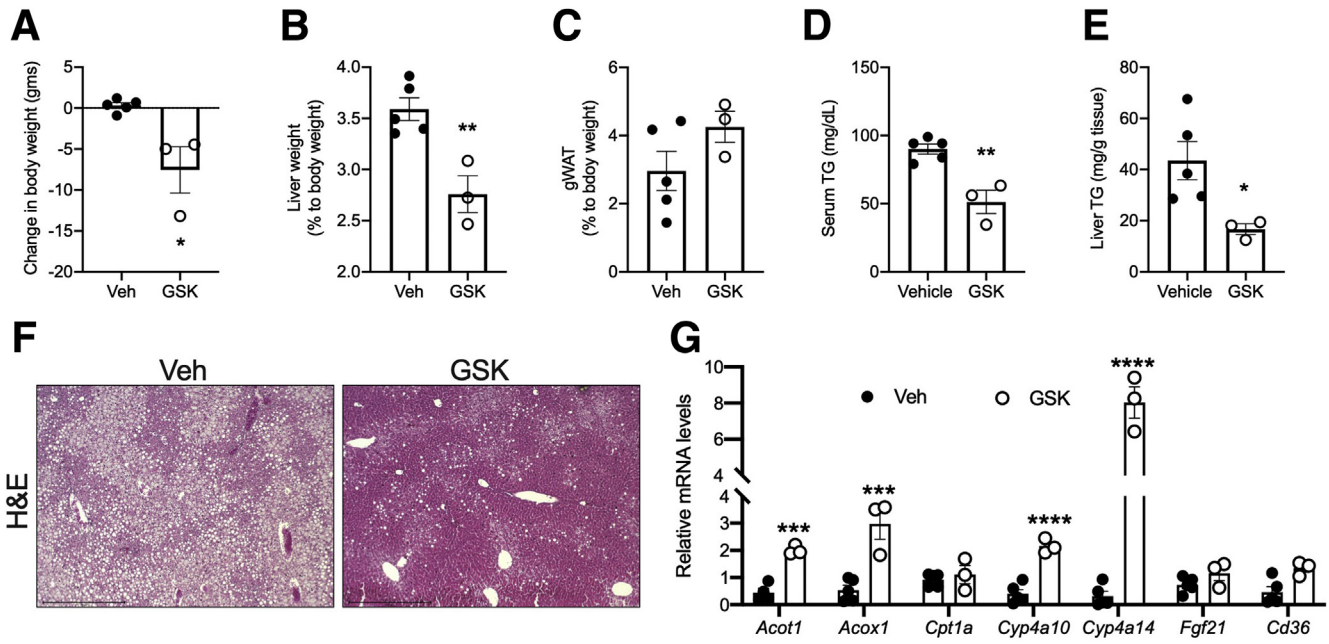

Figure 6. ERK inhibition attenuates diet-induced hepatic steatosis. C57BL6 male mice fed with 60% HFD for 8 weeks were treated with GSK at 3 mg/kg body weight for 5 days. On the day of euthanization, mice were treated with GSK, and tissues were collected 1 hour later. (*A*) Change in body weight, (*B*) percentage of liver weight, and (*C*) percentage of gonadal white adipose tissue (gWAT) in HFD-induced steatosis mice treated with or without GSK. (*D*) Serum and (*E*) liver triglycerides (*F*) H&E analysis in the livers of HFD-fed GSK-treated mice. Original magnification, ×20. (*G*) qPCR analysis for PPARα target genes in the livers of HFD-fed GSK-treated mice. Bar graphs are presented as mean standard error ± standard error of the mean. **P* < .05, ***P* < .01, ****P* < .001, *****P* < .0001as analyzed by two-tailed Student *t* test.

β-oxidation (Figure 7*B*). Fasting increases hepatic triglycerides partly because of the mobilization of fatty acids from adipose tissue, whereas refeeding decreases hepatic triglycerides because of the secretion of very low density lipoprotein triglycerides.[31,32] Therefore, we tested whether MEK-ERK signaling regulates hepatic lipid homeostasis in response to fasting-refeeding. GSK treatment did not affect the hepatic triglyceride levels under fasting (Figure 7*C*).[31,32] Intriguingly, MEK-ERK inhibition abrogated the refeeding-mediated decrease in hepatic triglycerides (Figure 7*C*). However, GSK treatment did not affect serum triglyceride levels during the fasting-refeeding regimen (Figure 7*D*). This suggests that MEK-ERK signaling plays a crucial role in postprandial hepatic lipid metabolism by regulating hepatic PPARα signaling.

Discussion

Chronic activation of hypoxia signaling leads to spontaneous steatohepatitis.[11,18] The present study shows that hypoxia signaling induces fatty liver by repressing PPARα signaling in an ERK-dependent manner. Our results also demonstrate that ERK inhibits ligand-dependent PPARα activation. We further show that inhibition of MEK-ERK signaling decreases hepatic steatosis in a model of diet-induced obesity. During fasting, PPARα-mediated fatty acid β-oxidation provides energy and substrates to support gluconeogenesis.[33] However, fatty acid β-oxidation genes decrease during the postprandial state, helping restore hepatic lipid levels and switch to carbohydrate metabolism. The absence of a switch in postprandial fatty acid β-oxidation may reduce carbohydrate utilization, resulting in hyperglycemia. Thus, the postprandial repression of fatty acid β-oxidation is critical in maintaining energy homeostasis and preventing insulin resistance and other metabolic dysfunctions.[34] Here we provide evidence that ERK plays an essential role in postprandial regulation of fatty oxidation genes by repressing PPARα.

HIF signaling, primarily HIF2α, was shown to induce dysregulation of hepatic lipid metabolism by inducing pexophagy. Although chloroquine is a nonselective autophagy inhibitor, our data show that inhibition of autophagy does not restore peroxisome or lipid homeostasis in the primary hepatocytes from mice with chronic HIF activation. HIF2α decreases the expression of fatty acid synthase in the liver.[14] Endogenous fatty acids act as a potent agonist of PPARα,[35] raising the possibility that HIF2α inhibits PPARα activity by decreasing the endogenous ligands. However, attenuation of the WY-mediated increase in PPARα target genes in $Vhl^{\Delta Hep}$ mice suggests that the decrease in endogenous ligands may not be responsible for decreasing PPARα signaling. We show that HIF2α induces lipid accumulation in hepatocytes by inhibiting PPARα signaling via the MEK-ERK–dependent mechanism.

Few studies have investigated the role of ERK in the regulation of PPARα by using cardiac hypertrophy models. Cardiac remodeling involves a switch in substrate utilization from fatty acid β-oxidation to glycolysis to reduce adenosine

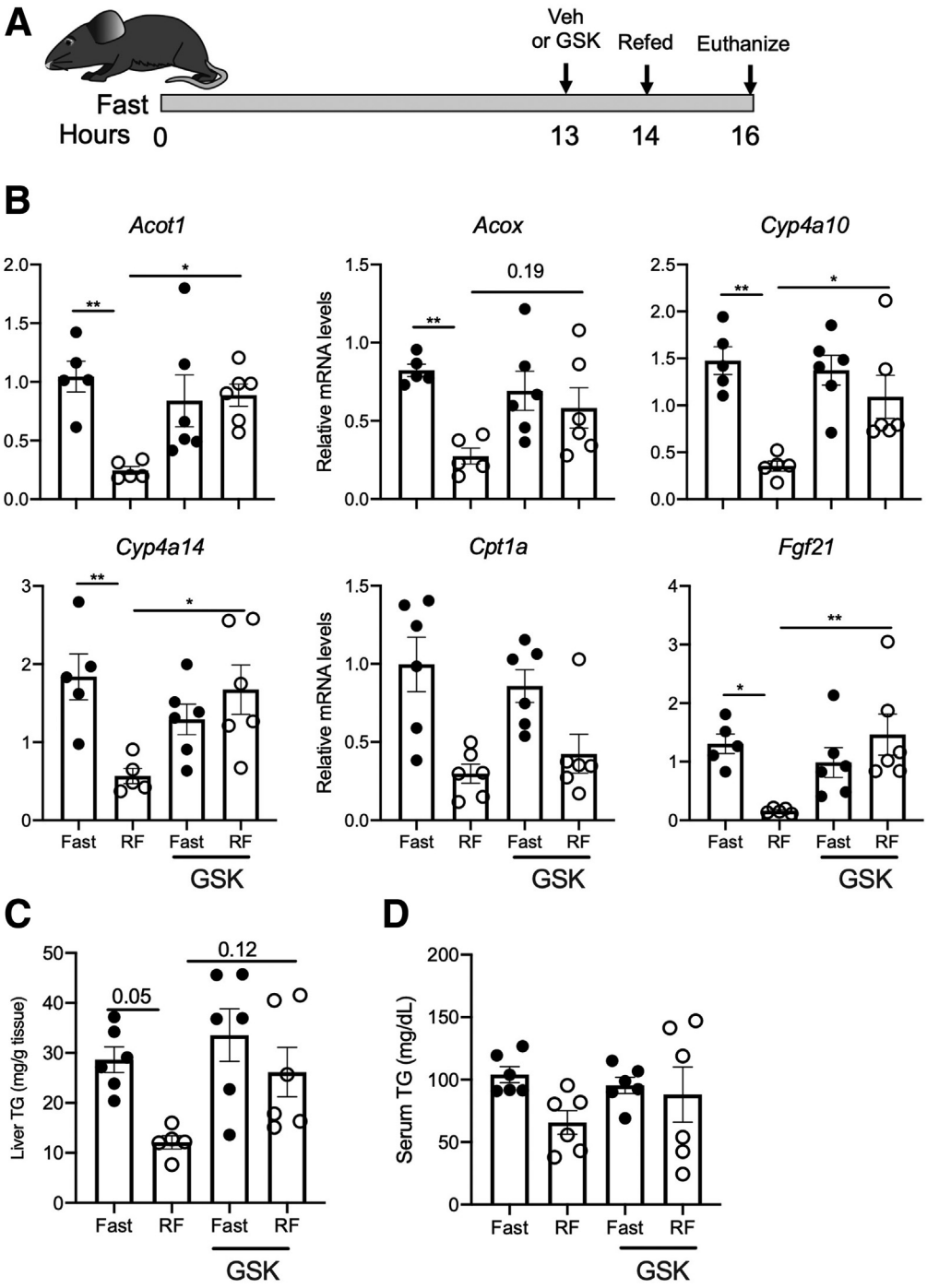

Figure 7. ERK inhibits PPARα during the refed state. (*A*) Schematic diagram of experimental design where overnight fasted and refed (fasted overnight and then refed) mice that were treated with vehicle or GSK (3 mg/kg body weight). (*B*) qPCR analysis of PPARα target genes in the livers of fasted and refed mice treated with or without GSK. (*C*) Liver and (*D*) serum triglycerides measured in the fasted and refed mice. Bar graphs are presented as mean standard error ± standard error of the mean. $^{*}P < .05$, $^{**}P < .01$ as analyzed by two-tailed Student *t* test. RF, refed.

triphosphate and oxygen consumption. ERK is involved in the metabolic switch by inhibiting fatty acid β-oxidation genes.[36,37] The present study shows that knockdown or activation of MEK-ERK signaling increases or decreases PPARα activity, respectively, suggesting that the MEK-ERK pathway regulates PPARα signaling in hepatocytes. Studies show that MEK1 induces nuclear export of PPARα, independent of ERK.[38] Moreover, PPARα has 3 potential ERK phosphorylation sites at Ser^{12}, Ser^{21}, and Ser^{77}, wherein phosphorylation at Ser^{12} and Ser^{21} but not Ser^{77} induces PPARα signaling.[27,39] Notably, phosphorylation at Ser^{84} inhibits PPARγ transcriptional activity.[40] Whether ERK inhibits PPARα activity by phosphorylating at Ser77 or via PPARα co-regulators needs further investigation.

Hepatic steatosis occurs because of an imbalance between fatty acid import/synthesis and export/catabolism in the liver.[41,42] Hepatic steatosis often leads to inflammation, insulin resistance, and fibrosis leading to nonalcoholic steatohepatitis.[43,44] There are no approved drugs for nonalcoholic steatohepatitis because of a poor understanding of the disease pathogenesis. Recent studies demonstrate that inhibition of hepatic PPARα is sufficient to promote

diet-induced hepatic steatosis.[30,45] This study shows that hepatic MEK-ERK could be targeted to activate PPARα-mediated fatty acid metabolism and thereby attenuate hepatic steatosis. Recent studies demonstrated that ERK inhibitors ameliorate insulin resistance in a diabetic mouse model by decreasing proinflammatory cytokines in the adipose tissue.[46–48] Our study provides a strong rationale for future investigations in determining whether MEK-ERK signaling could target fatty liver disease.

We also demonstrate the physiological relevance of MEK-ERK regulation of PPARα in metabolic homeostasis using a fasting-refeeding regimen. We show that inhibition of MEK-ERK does not affect PPARα signaling at the fasting state but abolishes postprandial repression of PPARα target genes. This could be due to lower activity of ERK during fasting to facilitate PPARα signaling,[49] wherein GSK treatment could not further augment the expression of fatty acid β-oxidation genes. Thus, we propose that MEK-ERK signaling is involved in the postprandial inhibition of fatty acid β-oxidation required for the switch in substrate utilization. Surprisingly, inhibition of MEK-ERK abolished the postprandial decrease in liver triglycerides. This suggests that MEK-ERK signaling could also control the postprandial release of hepatic triglyceride as very low density lipoprotein,[40,50] which requires further investigation.

Refeeding-induced liver hypoxia represses postprandial glucagon signaling.[6] One of the cellular adaptations to low oxygen is down-regulating pathways that consume oxygen. Because fatty acid β-oxidation is a highly oxygen-demanding process, hypoxia during the postprandial state may repress fatty acid β-oxidation as an adaptive mechanism to divert the available oxygen to essential cellular functions.[51] Also, decreasing fatty acid β-oxidation benefits in alleviating reactive oxygen species–mediated oxidative stress, especially under hypoxic conditions.[52] Because refeeding results in acute hepatic hypoxia, we speculate that hypoxia is involved in the postprandial repression of PPARα activity. However, sustained repression of fatty acid β-oxidation due to chronic hypoxia results in excessive accumulation of triglycerides in hepatocytes leading to the fatty liver.[6,8,9,17] Thus, a rheostatic regulation of HIF-ERK-PPARα appears to be critical for hepatic lipid homeostasis.

Methods

Animal Studies

Vhl$^{fl/fl}$ and *Vhl*$^{\Delta Hep}$ mice used in this study were described in an earlier article.[17] Briefly, mice that express a tamoxifen-inducible cre recombinase (Cre^{ERT2}) under the control of the albumin promoter were crossed with *Vhl*$^{fl/fl}$ to generate *Vhl*$^{\Delta Hep}$ mice. To conditionally knockout VHL in the hepatocytes, tamoxifen (Sigma-Aldrich, St Louis, MO; T5648) dissolved in corn oil was injected intraperitoneally (200 mg/kg body weight) for 2 consecutive days. Littermate *Vhl*$^{fl/fl}$ mice were used as controls. Mice were fed ad libitum with a regular chow diet and kept in a 12-hour dark-light cycle. For the fasting-refeeding experiments, the animals were fasted overnight, and 1 hour before killing or feeding, they were gavaged with the MEK inhibitor GSK1120212 (3 mg/kg body weight). GSK1120212 was dissolved in dimethyl sulfoxide and diluted with phosphate-buffered saline 1:10 and gavaged immediately. For the HFD experiments, C57BL/6J mice fed with a 60% HFD for 8 weeks were gavaged with the MEK inhibitor GSK1120212 (3 mg/kg body weight) for 5 days. All the experiments were conducted in accordance with relevant guidelines and regulations, and the animal experiments were approved by the Institutional Committee on the Use and Care of Animals at the University of Michigan.

Western Blot Analysis

Whole-cell lysates were prepared using radioimmunoprecipitation assay lysis buffer (50 mmol/L Tris pH 7.4, 150 mmol/L NaCl, 5 mmol/L EDTA, 1% NP-40) containing protease and phosphatase inhibitors (Sigma-Aldrich). Equal amounts of protein lysates were separated on a 10% sodium dodecyl sulfate–polyacrylamide gel electrophoresis and transferred to the nitrocellulose membrane. Membranes were blocked using 5% skim milk and probed with the specific antibody against LC3B (#2775S), pERK (#4370S), ERK (#4696S), actin (#4967L), catalase (#12980), and GAPDH (#97166S) from Cell Signaling Technology (Danvers, MA) and PPARα[18] (Abcam, Cambridge, UK; Ab126285) at 4°C for overnight. Horseradish peroxidase–conjugated secondary antibodies (anti-rabbit, #7074S and anti-mouse, 7076S) from Cell Signaling Technology were added for 1 hour, and the expression of proteins was assessed using ChemiDoc system (BioRad, Hercules, CA).

RNA Isolation and qPCR Analysis

Total RNA was isolated using Trizol reagent (Invitrogen, Carlsbad, CA) as per the manufacturer's instructions. One μg of RNA was reverse transcribed using Mu-MLV reverse transcriptase (Invitrogen). qPCR was performed using specific primers for mouse *Acot1*, forward: 5′-ATGGCAGCAGCTCCAGACTT-3′, reverse 5′-CCCAACCTCCAAACCATCAT-3′ *Acox1,* forward: 5′-TCGAAGCCAGCGTTACGAG-3′, reverse: 5′-ATCTCCGTCTGGGCGTAGG-3′ *Cpt1,* forward: 5′-CCATGTAAGGACGGGAGTGT-3′, reverse: 5′-TGCAGGCCCTACTATTCCTG-3′ *Fgf21,* forward: 5′-CTGCTGGGGGTCTACCAAG-3′ reverse: 5′-CTGCGCCTACCACTGTTCC-3′ *Cd36,* forward: 5′-CCTGCAAATGTCAGAGGAAA-3′, reverse: 5′-GCGACATGATTAATGGCACA-3′ *Cpt1a,* forward: 5′-CCAGGCTACAGTGGGACATT-3′, reverse: 5′-GAACTTGCCCATGTCCTTGT-3′ *Cyp4a10,* forward: 5′-GGAGCTCCAATGTCTGAGAAGAGT-3′, reverse: 5′-TCTCTGGAGTATTCTTCTGAAAAAGGT-3′ *Cyp4a14,* forward: 5′-TCTCTGGCTTTTCTGTACTTTGCTT-3′, reverse 5′-CAGAAAGATGAGATGACAGGACACA-3′ and *Actin,* forward: 5′-TATTGGCAACGAGCGGTTCC-3′, reverse: 5′-GGCATAGAGGTCTTTACGGATGT-3′ against target genes using SYBR green (Radiant Biologicals, Tampa, FL). Expression of genes was normalized to *Actin* or *Ppia,* and relative expression was determined using the cycle threshold method.

Primary Hepatocyte Isolation and Treatment

Primary hepatocytes from *Vhl*$^{\Delta Hep}$ and *Ppara*-null mice were isolated as described earlier.[53] Briefly, the abdominal cavity was opened in anesthetized mice, and the livers were perfused with 15 mL Earle's balanced salt solution containing 0.5 mmol/L EGTA via the portal vein, followed by perfusion with 15 mL Williams E medium containing 0.45 mg/mL collagenase type 1. Livers were then excised, and cells were scraped into Williams E medium with 10% fetal bovine serum and 1% antibiotics. Live cells were separated using Percoll gradient centrifugation. Primary hepatocytes were then plated at 0.1×10^6 cells/well in a 12-well plate or 0.2 1×10^6 cells/well in a 6-well plate. Two hours after plating, the medium was changed to fresh medium. For treating with fatty acids, bovine serum albumin–conjugated palmitic or oleic acid was added to the serum-free Williams E medium and incubated for various time points as indicated in the Figure legends. Primary hepatocytes were treated with GSK in serum-free medium for the indicated times.

Oil-Red-O Staining

For neutral lipid staining and quantification, primary hepatocytes were fixed with phosphate-buffered saline–buffered formalin for 10 minutes and then incubated with 0.5% oil-red-O in propylene glycol for 1 hour. Cells were washed once with 60% propylene glycol, rinsed with distilled water, and then counterstained with hematoxylin. Oil-red-O staining intensity was quantified by using a spectrophotometer (OD at 492) by adding 100% isopropanol to the stained wells or by analyzing H&E images using Image J 1.52q software (NIH, Bethesda, MD).

Liver Triglyceride Quantitation

Liver triglycerides were measured as described previously.[54] In brief, a known amount of liver tissue was homogenized in chloroform: methanol (2:1), followed by acidification with H_2SO_4. The organic phase containing the lipids was collected after centrifugation. The triglycerides from the organic phase and serum were measured using colorimetric Infinity Triglyceride Reagent (Fisher Scientific, Waltham, MA).

Adenovirus miR-ERK1/2

The adenovirus miR-ERK1/2 producing process was carried out in accordance with the protocol from ViraPower Adenoviral Expression System, BLOCK-iT Pol II miR RNAi Expression Vector Kit with EmGFP, pENTR Directional TOPO Cloning kits, GATEWAY LR clonase II MS Enzyme MIX, and Gateway BP Clonase II Enzyme mix. In brief, miRNA sequence and oligos for Erk1/2 were designed by BLOCK-iT RNAi Designer. To generate a double-stranded oligo, the top and bottom strand oligo for Erk1/2 (top, 5′-TGC TGA GCA GAT GTG GTC ATT GCT CAG TTT TGG CCA CTG ACT GAC TGA GCA ATC CAC ATC TGC T-3′, and bottom, 5′-CCT GAG CAG ATG TGG ATT GCT CAG TCA GTC AGT GGC CAA AAC TGA GCA ATG ACC ACA TCT GCT C-3′) were annealed in the following annealing reaction (95°C for 4 minutes and then at 4°C for 10 minutes). The annealed fragment was cloned into pcDNA6.2-GW EmGFP-miR to generate pcDNA6.2-miR-Erk1/2. To make the adenovirus miR-Erk1/2, BP and LR reactions were performed using Gateway cloning. The titer of recombinant adenoviruses was determined using Adeno-X Rapid Titer Kit. Recombinant adenovirus miR-LacZ (Ad-LacZ) was infected in the same manner as a control. Adeno-MEK-ERK-LA virus was a gift from Dr Michael Simons from Yale University, wherein MEK1-ERK2 fusion construct was subcloned into adenoviral pAd/CMV/V5-DEST vector.[55] Five hours after plating, cells were incubated in medium containing adenovirus vectors (20 MOI). Twenty hours after adenovirus infections, cells were incubated in serum-free William E medium for 2 hours and then treated with 0.5 μmol/L GSK for indicated amounts of time in respective Figure legends.

Statistical Analysis

The experimental data were analyzed using GraphPad Prism 8 software (San Diego, CA) and presented as mean ± standard error of the mean. For analysis of statistical significance between 2 groups, a two-tailed unpaired Student *t* test was used. For analysis of statistical significance between 3 or more groups, one-way analysis of variance with Tukey multiple comparisons was used. All the in vitro experiments were carried out in triplicates, and the graphs were presented as dot bar graphs with each of the biological replicates. $P > .05$ was considered significant.

References

1. Wakil SJ, Abu-Elheiga LA. Fatty acid metabolism: target for metabolic syndrome. J Lipid Res 2009; 50(Suppl):S138–S143.
2. Rui L. Energy metabolism in the liver. Compr Physiol 2014;4:177–197.
3. Demarquoy J, Le Borgne F. Crosstalk between mitochondria and peroxisomes. World J Biol Chem 2015; 6:301–309.
4. Poirier Y, Antonenkov VD, Glumoff T, Hiltunen JK. Peroxisomal β-oxidation: a metabolic pathway with multiple functions. Biochim Biophys Acta 2006; 1763:1413–1426.
5. Yoon M. The role of PPARα in lipid metabolism and obesity: focusing on the effects of estrogen on PPARα actions. Pharmacol Res 2009;60:151–159.
6. Ramakrishnan SK, Zhang H, Takahashi S, Centofanti B, Periyasamy S, Weisz K, Chen Z, Uhler MD, Rui L, Gonzalez FJ, Shah YM. HIF2α is an essential molecular brake for postprandial hepatic glucagon response independent of insulin signaling. Cell Metab 2016; 23:505–516.
7. Li D, Du Y, Yuan X, Han X, Dong Z, Chen X, Wu H, Zhang J, Xu L, Han C, Zhang M, Xia Q. Hepatic hypoxia-inducible factors inhibit PPARα expression to exacerbate acetaminophen induced oxidative stress and hepatotoxicity. Free Radic Biol Med 2017;110:102–116.
8. Rankin EB, Rha J, Selak MA, Unger TL, Keith B, Liu Q, Haase VH. Hypoxia-inducible factor 2

regulates hepatic lipid metabolism. Mol Cell Biol 2009;29:4527–4538.
9. Qu A, Taylor M, Xue X, Matsubara T, Metzger D, Chambon P, Gonzalez FJ, Shah YM. Hypoxia-inducible transcription factor 2α promotes steatohepatitis through augmenting lipid accumulation, inflammation, and fibrosis. Hepatology 2011;54:472–483.
10. Ratcliffe PJ. HIF-1 and HIF-2: working alone or together in hypoxia? J Clin Invest 2007;117:862–865.
11. Nath B, Szabo G. Hypoxia and hypoxia inducible factors: diverse roles in liver diseases. Hepatology 2012; 55:622–633.
12. Wilson GK, Tennant DA, McKeating JA. Hypoxia inducible factors in liver disease and hepatocellular carcinoma: current understanding and future directions. J Hepatol 2014;61:1397–1406.
13. Majmundar AJ, Wong WJ, Simon MC. Hypoxia-inducible factors and the response to hypoxic stress. Mol Cell 2010;40:294–309.
14. Morello E, Sutti S, Foglia B, Novo E, Cannito S, Bocca C, Rajsky M, Bruzzi S, Abate ML, Rosso C, Bozzola C, David E, Bugianesi E, Albano E, Parola M. Hypoxia-inducible factor 2α drives nonalcoholic fatty liver progression by triggering hepatocyte release of histidine-rich glycoprotein. Hepatology 2018;67:2196–2214.
15. Feng Z, Zou X, Chen Y, Wang H, Duan Y, Bruick RK. Modulation of HIF-2α PAS-B domain contributes to physiological responses. Proc Natl Acad Sci U S A 2018; 115:13240–13245.
16. Tirosh O. Hypoxic signaling and cholesterol lipotoxicity in fatty liver disease progression. Oxid Med Cell Longev 2018;2018:2548154.
17. Ramakrishnan SK, Taylor M, Qu A, Ahn SH, Suresh MV, Raghavendran K, Gonzalez FJ, Shah YM. Loss of von Hippel-Lindau protein (VHL) increases systemic cholesterol levels through targeting hypoxia-inducible factor 2alpha and regulation of bile acid homeostasis. Mol Cell Biol 2014;34:1208–1220.
18. Chen J, Chen J, Fu H, Li Y, Wang L, Luo S, Lu H. Hypoxia exacerbates nonalcoholic fatty liver disease via the HIF-2α/PPARα pathway. Am J Physiol Endocrinol Metab 2019;317:E710–E722.
19. Walter KM, Schonenberger MJ, Trotzmuller M, Horn M, Elsasser HP, Moser AB, Lucas MS, Schwarz T, Gerber PA, Faust PL, Moch H, Kofeler HC, Krek W, Kovacs WJ. Hif-2α promotes degradation of mammalian peroxisomes by selective autophagy. Cell Metab 2014;20:882–897.
20. Maxwell PH, Wiesener MS, Chang GW, Clifford SC, Vaux EC, Cockman ME, Wykoff CC, Pugh CW, Maher ER, Ratcliffe PJ. The tumour suppressor protein VHL targets hypoxia-inducible factors for oxygen-dependent proteolysis. Nature 1999;399:271–275.
21. Bosc C, Broin N, Fanjul M, Saland E, Farge T, Courdy C, Batut A, Masoud R, Larrue C, Skuli S, Espagnolle N, Pages JC, Carrier A, Bost F, Bertrand-Michel J, Tamburini J, Recher C, Bertoli S, Mansat-De Mas V, Manenti S, Sarry JE, Joffre C. Autophagy regulates fatty acid availability for oxidative phosphorylation through mitochondria-endoplasmic reticulum contact sites. Nat Commun 2020;11:4056.
22. Wang J, Han SL, Lu DL, Li LY, Limbu SM, Li DL, Zhang ML, Du ZY. Inhibited lipophagy suppresses lipid metabolism in Zebrafish liver cells. Front Physiol 2019; 10:1077.
23. Heppner KM, Habegger KM, Day J, Pfluger PT, Perez-Tilve D, Ward B, Gelfanov V, Woods SC, DiMarchi R, Tschop M. Glucagon regulation of energy metabolism. Physiol Behav 2010;100:545–548.
24. Petersen MC, Vatner DF, Shulman GI. Regulation of hepatic glucose metabolism in health and disease. Nat Rev Endocrinol 2017;13:572–587.
25. Longuet C, Sinclair EM, Maida A, Baggio LL, Maziarz M, Charron MJ, Drucker DJ. The glucagon receptor is required for the adaptive metabolic response to fasting. Cell Metab 2008;8:359–371.
26. Purushotham A, Schug TT, Xu Q, Surapureddi S, Guo X, Li X. Hepatocyte-specific deletion of SIRT1 alters fatty acid metabolism and results in hepatic steatosis and inflammation. Cell Metab 2009;9:327–338.
27. Burns KA, Vanden Heuvel JP. Modulation of PPAR activity via phosphorylation. Biochim Biophys Acta 2007; 1771:952–960.
28. Gardner OS, Dewar BJ, Earp HS, Samet JM, Graves LM. Dependence of peroxisome proliferator-activated receptor ligand-induced mitogen-activated protein kinase signaling on epidermal growth factor receptor transactivation. J Biol Chem 2003;278:46261–46269.
29. Lefebvre P, Chinetti G, Fruchart JC, Staels B. Sorting out the roles of PPAR α in energy metabolism and vascular homeostasis. J Clin Invest 2006;116:571–580.
30. Montagner A, Polizzi A, Fouche E, Ducheix S, Lippi Y, Lasserre F, Barquissau V, Regnier M, Lukowicz C, Benhamed F, Iroz A, Bertrand-Michel J, Al Saati T, Cano P, Mselli-Lakhal L, Mithieux G, Rajas F, Lagarrigue S, Pineau T, Loiseau N, Postic C, Langin D, Wahli W, Guillou H. Liver PPARα is crucial for whole-body fatty acid homeostasis and is protective against NAFLD. Gut 2016;65:1202–1214.
31. Donepudi AC, Boehme S, Li F, Chiang JY. G-protein-coupled bile acid receptor plays a key role in bile acid metabolism and fasting-induced hepatic steatosis in mice. Hepatology 2017;65:813–827.
32. Pantaleao LC, Murata G, Teixeira CJ, Payolla TB, Santos-Silva JC, Duque-Guimaraes DE, Sodre FS, Lellis-Santos C, Vieira JC, de Souza DN, Gomes PR, Rodrigues SC, Anhe GF, Bordin S. Prolonged fasting elicits increased hepatic triglyceride accumulation in rats born to dexamethasone-treated mothers. Sci Rep 2017; 7:10367.
33. Chakravarthy MV, Pan Z, Zhu Y, Tordjman K, Schneider JG, Coleman T, Turk J, Semenkovich CF. New" hepatic fat activates PPARα to maintain glucose, lipid, and cholesterol homeostasis. Cell Metab 2005; 1:309–322.
34. Bechmann LP, Hannivoort RA, Gerken G, Hotamisligil GS, Trauner M, Canbay A. The interaction of hepatic lipid and glucose metabolism in liver diseases. J Hepatol 2012;56:952–964.
35. Chakravarthy MV, Lodhi IJ, Yin L, Malapaka RR, Xu HE, Turk J, Semenkovich CF. Identification of a

physiologically relevant endogenous ligand for PPARα in liver. Cell 2009;138:476–488.
36. Sack MN, Disch DL, Rockman HA, Kelly DP. A role for Sp and nuclear receptor transcription factors in a cardiac hypertrophic growth program. Proc Natl Acad Sci U S A 1997;94:6438–6443.
37. Barger PM, Brandt JM, Leone TC, Weinheimer CJ, Kelly DP. Deactivation of peroxisome proliferator-activated receptor-α during cardiac hypertrophic growth. J Clin Invest 2000;105:1723–1730.
38. el Azzouzi H, Leptidis S, Bourajjaj M, van Bilsen M, da Costa Martins PA, De Windt LJ. MEK1 inhibits cardiac PPARα activity by direct interaction and prevents its nuclear localization. PLoS One 2012;7:e36799.
39. Juge-Aubry CE, Hammar E, Siegrist-Kaiser C, Pernin A, Takeshita A, Chin WW, Burger AG, Meier CA. Regulation of the transcriptional activity of the peroxisome proliferator-activated receptor alpha by phosphorylation of a ligand-independent trans-activating domain. J Biol Chem 1999;274:10505–10510.
40. Adams M, Reginato MJ, Shao D, Lazar MA, Chatterjee VK. Transcriptional activation by peroxisome proliferator-activated receptor γ is inhibited by phosphorylation at a consensus mitogen-activated protein kinase site. J Biol Chem 1997;272:5128–5132.
41. Ipsen DH, Lykkesfeldt J, Tveden-Nyborg P. Molecular mechanisms of hepatic lipid accumulation in non-alcoholic fatty liver disease. Cell Mol Life Sci 2018; 75:3313–3327.
42. Cheung O, Sanyal AJ. Abnormalities of lipid metabolism in nonalcoholic fatty liver disease. Semin Liver Dis 2008; 28:351–359.
43. Polyzos SA, Kountouras J, Mantzoros CS. Obesity and nonalcoholic fatty liver disease: from pathophysiology to therapeutics. Metabolism 2019;92:82–97.
44. Younossi ZM. Non-alcoholic fatty liver disease: a global public health perspective. J Hepatol 2019;70:531–544.
45. Stec DE, Gordon DM, Hipp JA, Hong S, Mitchell ZL, Franco NR, Robison JW, Anderson CD, Stec DF, Hinds TD Jr. Loss of hepatic PPARα promotes inflammation and serum hyperlipidemia in diet-induced obesity. Am J Physiol Regul Integr Comp Physiol 2019; 317:R733–R745.
46. Ozaki KI, Awazu M, Tamiya M, Iwasaki Y, Harada A, Kugisaki S, Tanimura S, Kohno M. Targeting the ERK signaling pathway as a potential treatment for insulin resistance and type 2 diabetes. Am J Physiol Endocrinol Metab 2016;310:E643–E651.
47. Banks AS, McAllister FE, Camporez JP, Zushin PJ, Jurczak MJ, Laznik-Bogoslavski D, Shulman GI, Gygi SP, Spiegelman BM. An ERK/Cdk5 axis controls the diabetogenic actions of PPARγ. Nature 2015; 517:391–395.
48. Khan AS, Subramaniam S, Dramane G, Khelifi D, Khan NA. ERK1 and ERK2 activation modulates diet-induced obesity in mice. Biochimie 2017;137:78–87.
49. Jiao P, Feng B, Li Y, He Q, Xu H. Hepatic ERK activity plays a role in energy metabolism. Mol Cell Endocrinol 2013;375:157–166.
50. Atkinson BJ, Griesel BA, King CD, Josey MA, Olson AL. Moderate GLUT4 overexpression improves insulin sensitivity and fasting triglyceridemia in high-fat diet-fed transgenic mice. Diabetes 2013;62:2249–2258.
51. Formenti F, Constantin-Teodosiu D, Emmanuel Y, Cheeseman J, Dorrington KL, Edwards LM, Humphreys SM, Lappin TR, McMullin MF, McNamara CJ, Mills W, Murphy JA, O'Connor DF, Percy MJ, Ratcliffe PJ, Smith TG, Treacy M, Frayn KN, Greenhaff PL, Karpe F, Clarke K, Robbins PA. Regulation of human metabolism by hypoxia-inducible factor. Proc Natl Acad Sci U S A 2010;107:12722–12727.
52. Schonfeld P, Wieckowski MR, Lebiedzinska M, Wojtczak L. Mitochondrial fatty acid oxidation and oxidative stress: lack of reverse electron transfer-associated production of reactive oxygen species. Biochim Biophys Acta 2010;1797:929–938.
53. Li WC, Ralphs KL, Tosh D. Isolation and culture of adult mouse hepatocytes. Methods Mol Biol 2010; 633:185–196.
54. Mooli RGR, Pavan Kumar C, Mahesh M, Sravan Kumar M, Mullapudi Venkata S, Putcha UK, Vajreswari A, Jeyakumar SM. Vitamin A deficiency suppresses high fructose-induced triglyceride synthesis and elevates resolvin D1 levels. Biochim Biophys Acta 2016;1861:156–165.
55. Ren B, Deng Y, Mukhopadhyay A, Lanahan AA, Zhuang ZW, Moodie KL, Mulligan-Kehoe MJ, Byzova TV, Peterson RT, Simons M. ERK1/2-Akt1 crosstalk regulates arteriogenesis in mice and zebrafish. J Clin Invest 2010;120:1217–1228.

Received August 5, 2020. Accepted March 17, 2021.

Correspondence
Address correspondence to: Yatrik M. Shah, PhD, University of Michigan, Molecular and Integrative Physiology, 1301 East Catherine Street, 7712B Medical Science II, Ann Arbor, Michigan 48109. e-mail: shahy@umich.edu; fax: (734) 936-8813 or Sadeesh K. Ramakrishnan, PhD, Division of Endocrinology and Metabolism, Department of Medicine, University of Pittsburgh, Pittsburgh, Pennsylvania. e-mail: ramaks@pitt.edu; fax: (412) 648-3290.

CRediT Authorship Contributions
Raja Gopal Reddy Mooli, PhD (Data curation: Lead; Formal analysis: Supporting; Investigation: Supporting; Methodology: Supporting; Validation: Supporting; Writing – original draft: Lead; Writing – review & editing: Lead)
Jessica Rodriguez (Investigation: Supporting)
Shogo Takahashi (Data curation: Lead; Formal analysis: Lead; Investigation: Lead; Writing – original draft: Supporting; Writing – review & editing: Supporting)
Sumeet Solanki, PhD (Methodology: Supporting)
Frank J. Gonzalez (Supervision: Supporting; Writing – original draft: Supporting; Writing – review & editing: Supporting)
Sadeesh Kumar Ramakrishnan (Conceptualization: Lead; Data curation: Lead; Funding acquisition: Lead; Investigation: Lead; Writing – original draft: Lead; Writing – review & editing: Lead)
Yatrik M. Shah (Conceptualization: Lead; Funding acquisition: Lead; Supervision: Lead; Writing – original draft: Lead; Writing – review & editing: Lead)

Conflicts of interest
The authors disclose no conflicts.

Funding
Supported by the National Institute of Diabetes and Digestive and Kidney Diseases (DK110537) and the Pittsburgh Liver Research Center Pilot and Feasibility grant (P30DK120531) to S.K.R, NIH grants CA148828 and DK095201 to Y.M.S, and the National Cancer Institute Intramural Research Program to Frank J. Gonzalez.